E-ELT PROGRAMME

MICADO Phase A
System Overview

Document: E-TRE-MCD-561-0009

Issue: 2.0

Date: 22.10.09

Author(s)	R. Davies T. Herbst M. Thiel
Proj. Manager	R. Davies

Name	Date & Signature

MICADO
Consortium

MICADO PHASE A

SYSTEM OVERVIEW

Doc: E-TRE-MCD-561-0009
Issue: 2.0
Date: 22.10.09
Page 2 of 30

CHANGE RECORD

ISSUE	DATE	SECTION/PAGE AFFECTED	REASON/ REMARKS
1		All	First issue
1.1	22.12.08	Document Name, Sec 3	Updated according to RIXs 2 and 51 from Phase A1 review
2.0	22.10.09	All	Complete update for Phase A

MICADO
Consortium

MICADO PHASE A

SYSTEM OVERVIEW

Doc: E-TRE-MCD-561-0009
Issue: 2.0
Date: 22.10.09
Page 3 of 30

TABLE OF CONTENTS

MICADO
Consortium

MICADO PHASE A

SYSTEM OVERVIEW

Doc: E-TRE-MCD-561-0009
Issue: 2.0
Date: 22.10.09
Page 4 of 30

ABBREVIATIONS AND ACRONYMS

AO	adaptive optics
CAD	computer aided design
CAE	computer aided engineering
ECSS	European Cooperation for Space Standardization
E-ELT	European Extremely Large Telescope
ESO	European Southern Observatory
FDR	Final Design Review
FTE	Full Time Equivalent (year)
GLAO	ground layer adaptive optics
GMT	Giant Magellan Telescope
JWST	James Web Space Telescope
LESIA	Laboratoire d'Etudes Spatiales et Instrumentations pour l'Astrophysique
LTAO	laser tomography adaptive optics
MAIT	Manufacture, Assembly, Integration, Test
MAORY	Multi-conjugate Adaptive Optics Relay
MCAO	multi-conjugate adaptive optics
MICADO	Multi-adaptive optics Imaging Camera for Deep Observations
MPE	Max-Planck-Institut für extraterrestrische Physik
MPIA	Max-Planck-Institut für Astronomie
NOVA	Nederlandse Onderzoekschool voor Astronomie
OAPD	Osservatorio Astronomico di Padova
PAE	Preliminary Acceptance in Europe
PAO	Preliminary Acceptance at the Observatory
PA/QA	Product Assurance / Quality Assurance
PDR	Preliminary Design Review
PSF	Point Spread Function
RTD	Real Time Display
SCAO	single-conjugate adaptive optics
TMT	Thirty Meter Telescope
USM	Universitäts-Sternwarte München
WP	Workpackage

MICADO
Consortium

MICADO PHASE A

SYSTEM OVERVIEW

Doc: E-TRE-MCD-561-0009
Issue: 2.0
Date: 22.10.09
Page 5 of 30

1 APPLICABLE AND REFERENCE DOCUMENTS

1.1 Applicable Documents

The following applicable documents form a part of the present document to the extent specified herein. In the event of conflict between applicable documents and the content of the present document, the present document shall be taken as superseding.

AD1 Common definitions and acronyms , E-ESO-SPE-313-0066, Issue 1

AD2 E-ELT Interfaces for Scientific Instruments, E-TRE-ESO-586-0252, issue 1

AD3 Call for Proposal For a Phase A Study of a High Angular Resolution Camera for the E-ELT, Specifications of the Instrument to be studied, E-ESO-SPE-561-0097, v2.0

AD4 Statement of Work for the Phase A Design of MICADO, E-SOW-ESO-561-0127, v1.0

AD5 Properties and Cost of Reference Detectors, Technical Note INS-2009/02

1.2 Reference Documents

RD1 Proposal "MICADO: the MCAO Imaging Camera for Deep Observations", 12 Nov 2007, in response to the call CFP/ESO/07/17768/LCO

RD2 MICADO Instrument Development and Management Plan, E-PLA-MCD-561-0020, v1.0

RD3 MICADO Scientific Analysis Report, E-TRE-MCD-561-0007, v2.0

RD4 MICADO Design Trade-Off and Risk Assessment, E-TRE-MCD-561-0010, v2.0

RD5 MICADO Opto-Mechanics Design and Analysis, E-TRE-MCD-561-0011, v5.0

RD6 MICADO Control Electronics Design, E-TRE-MCD-561-0013, v1.0

RD7 MICADO Top Level Instrument Software User Requirements, E-TRE-MCD-561-001, v1.0

RD8 MICADO Top Level Data Reduction User Requirements, E-TRE-MCD-561-0024, v1.0

RD9 MICADO Phase A Photometric Study, E-TRE-MCD-561-0023, v1.0

RD10 MICADO Single Conjugate Adaptive Optics Module, E-TRE-MCD-561-0022, v1.0

RD11 MICADO Compliance Matrix, E-TRE-MCD-561-0008, v2.0

RD12 MICADO-MAORY Phase A Interface Specification, E-SPE-MCD-561-0014, v1.0

RD13 MICADO-EELT Phase A Interface Information and Requests, E-SPE-MCD-561-0015, v1.0

MICADO
Consortium

MICADO PHASE A

SYSTEM OVERVIEW

Doc: E-TRE-MCD-561-0009
Issue: 2.0
Date: 22.10.09
Page 6 of 30

2   SCOPE

This document summarises the design concept that was selected by the consortium following science and technical trade-off studies, and approved for further study at the Phase A1 review. It summarises the key features of the optical, mechanical, and cryogenic design. In addition it outlines the MAIT plan and describes the Operational Concept for the instrument.

3   INSTRUMENT DESCRIPTION

3.1   General Concept

The design of MICADO has been developed by combining the results and conclusions from parallel scientific and technical trade-off studies (see the Design Trade-Off and Risk Assessment, RD4). These have resulted in a concept for the camera comprising purely reflective optics that images a contiguous field, having a ~75arcsec diagonal size, onto a focal plane. The focal plane is tiled with detectors, and provides 16000×16000 pixels at a scale of 3mas/pixel. As a baseline we adopt the HAWAII-4RG (with a 15μm pixel size), which has been developed to meet the stringent requirements of space astrometry. The combination of fixed monolithic optics, a single fixed mount for the focal plane array, and a gravity invariant rotation will significantly enhance the astrometric stability of the camera compared to other designs, as well as simplifying the associated mechanics. The design allows for a large wheel with space for 20 filters, providing a high degree of flexibility for imaging projects. Both the filter wheels, as well as the focal plane mechanism, are supported and driven at their rim, lessening the torque requirements on the mechanisms.
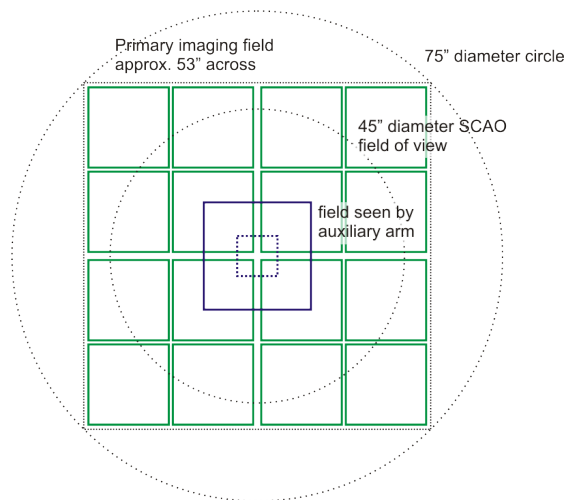

Figure 1: illustration showing how the focal plane will be divided in MICADO. The main imaging field is approximately 53"×53" and will be imaged at a scale of 3mas/pixel by an array of 4×4 HAWAII-4RG detectors. A selection mechanism will enable one to pick off a smaller field for the auxiliary arm.

MICADO
Consortium

MICADO PHASE A

SYSTEM OVERVIEW

Doc: E-TRE-MCD-561-0009
Issue: 2.0
Date: 22.10.09
Page 7 of 30

In addition to the primary imaging arm, MICADO has an auxiliary arm that can be selected by moving in a single mirror on a rotation stage. This arm has a separate filter wheel, providing space for an additional 20 filters, and requires only 1 additional HAWAII-4RG detector. In the current design, the auxiliary arm provides 2 important complementary capabilities: (i) a smaller 1.5mas pixel scale over a 6"x6" field of view, which is crucial for accurate astrometry in the most extremely crowded fields; (ii) a 4mas pixel scale for slit spectroscopy (the slit mask being located in the input focal plane mechanism) using R~3000-5000 grisms.
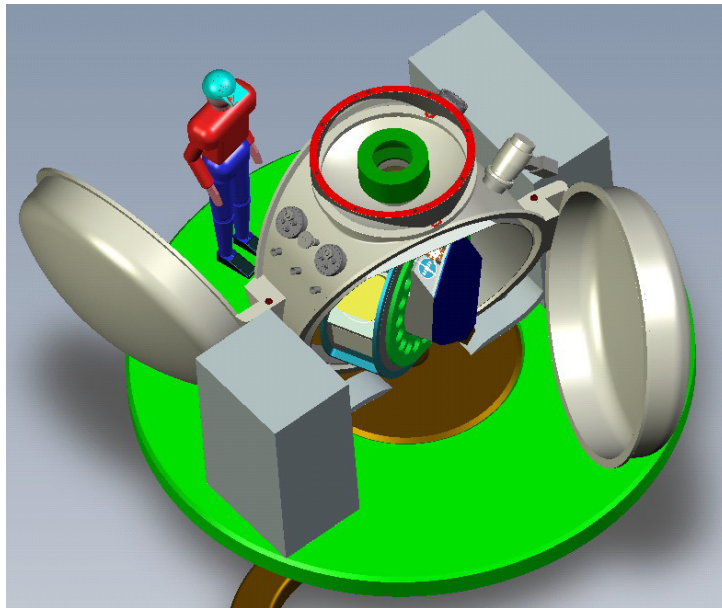

Figure 2: Overview of MICADO as it will be at the telescope. The mechanical interface to the AO systems is the red mounting ring on the top side. Access to all key systems is provided through 2 large doors in the cryostat, and facilitated because the optics mount is slightly rotated with respect to the cryostat. The electronics are mounted on a co-rotating platform that rests on the Nasmyth platform and also provides the cable-wrap for external supplies.

While MICADO achieves superb wide-field performance with the MCAO module MAORY, in its first phase MICADO will be combined with an internal SCAO module. As this simple on-axis, natural guide star mode sets low requirements on the telescope and AO performance (no lasers), MICADO+SCAO thus is an optimum choice for demonstrating the scientific capabilities of the E-ELT at first light. Since the E-ELT baseline is that SCAO wavefront sensing capability is not provided to the instruments by the telescope, the consortium has included the study of such a module. The optical relay and support structure have been designed so that the interface between MICADO and the SCAO module is the same as that with MAORY. Furthermore, they can in principle also be used to interface MICADO to other AO systems such as ATLAS.
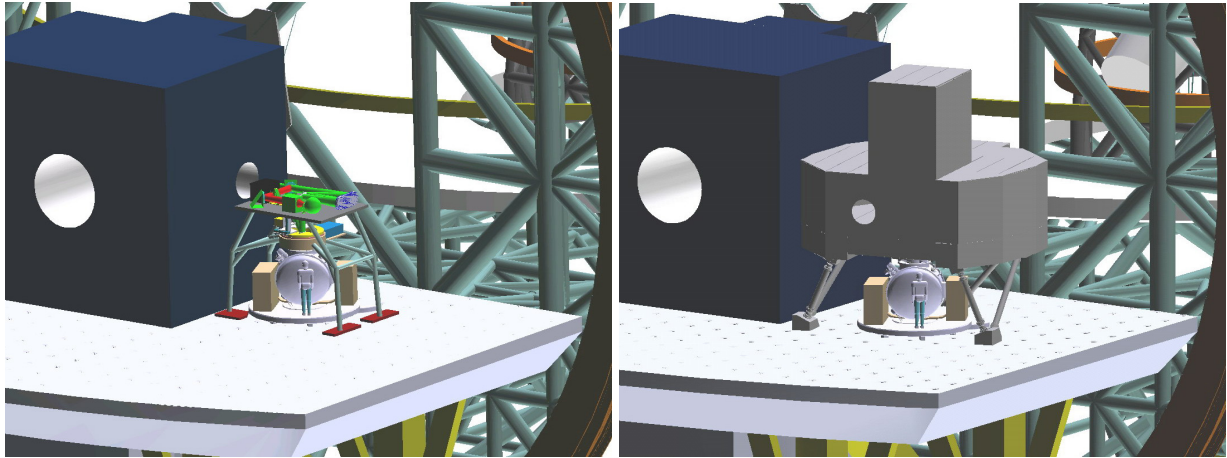
MICADO
Consortium

MICADO P*HASE* A

S*YSTEM* O*VERVIEW*

Doc: E-TRE-MCD-561-0009
Issue: 2.0
Date: 22.10.09
Page 8 of 30

Figure 3: View of MICADO as it will be mounted in a gravity invariant orientation under the SCAO module (left) and under MAORY (right). For the SCAO module, the relay optics is mounted on the upper optical table together with the calibration unit (both will be covered).

3.2   Optics

As shown in Figure 4 the MICADO optics comprises 3 sub-systems: the common path, the primary arm, and the auxiliary arm.

3.2.1 Common Path

The tunable ADC (not shown in the figure) consists of 2 pairs of ZnSe/ZnS prisms, which can be rotated to provide a dispersion correction that can be optimised to the observational band. It is located as far in front of (i.e. 500mm from) the input focal plane as possible. This is to minimize its impact on the optical quality by enabling thinner prisms with smaller wedge angles to be used. In its current location (warm and right against the interface to MAORY), the performance is just acceptable. However, this location is not optimal and during Phase B other options, such as locating it at an appropriate pupil plane within MAORY, will be addressed. In addition, if the E-ELT has an ADC, it may be possible to simplify that provided by MICADO.

Both arms use an off-axis parabola for collimation. However, the sizes and locations of the parabolae are different, and so the primary arm used a fixed mirror, while use of the auxiliary arm requires an alternative mirror to be rotated into position. In both cases, to keep the optical system compact, the light is reflected in both directions from a large fold mirror. Separate fixed pick-off fold mirrors then direct the light out of the common path to opposite sides of the instrument. The collimator creates a pupil image just after this fold mirror, where a large filter wheel is located. The maximum circular diameter of the pupil is 100.5mm; however, in order to block unwanted background (the pupil has a shape that depends slightly on field position), the coldstop has to be undersized at 99mm diameter.
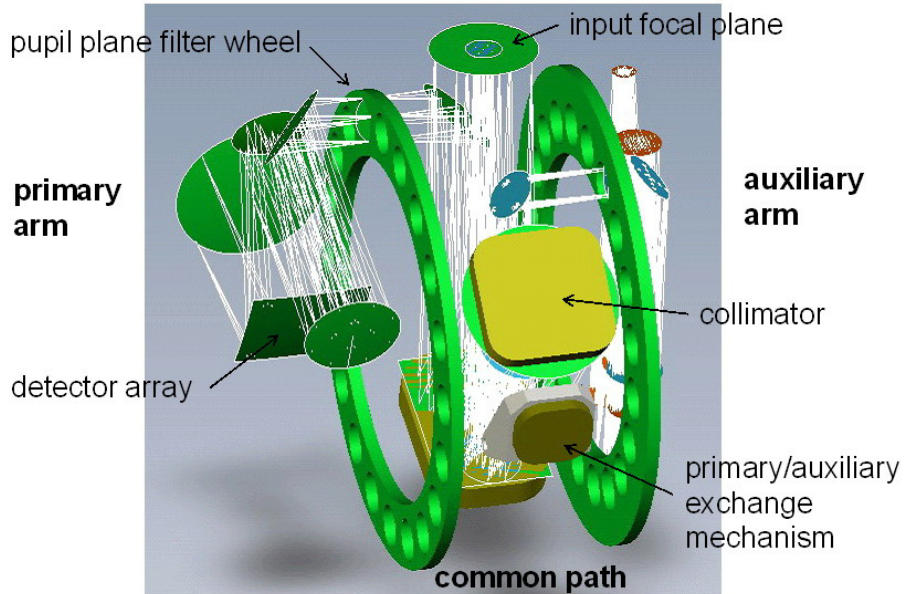
MICADO
Consortium

MICADO PHASE A

SYSTEM OVERVIEW

Doc: E-TRE-MCD-561-0009
Issue: 2.0
Date: 22.10.09
Page 9 of 30

Figure 4: Overview of MICADO optics, which comprises the common path (ADC (not shown) and collimator), the primary arm, and the auxiliary arm.

3.2.2 Primary Arm

The basic design of the primary arm is shown in Figure 5.
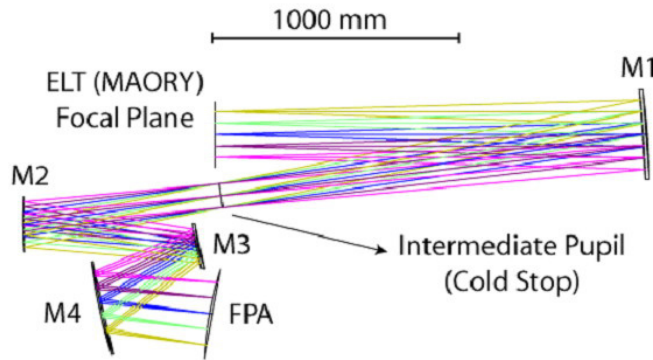
Figure 5: working mirrors for the primary arm. M1 is the parabolic collimator; M2-M4 re-image the field onto the focal plane array. Additional flat fold mirrors (within the collimator and immediately after the pupil) are needed to keep the instrument compact.

The salient points for this design are summarised in Table 1.

Table 1: characteristics of the optical design of the primary arm

Throughput	61-70% for Y-K bands (i.e. 39-45% including telescope & AO)
FoV & pixel scale	53"×53" at 3mas/pixel
Filters	Single filter wheel with 20 positions for filters

MICADO
Consortium

MICADO PHASE A

SYSTEM OVERVIEW

Doc: E-TRE-MCD-561-0009
Issue: 2.0
Date: 22.10.09
Page 10 of 30

Image Quality	Nominal strehl ratio at 1μm is >89% across the whole field.
Distortion	1.2% across the whole field of view
Ghosts	The reflective optics do not create ghosts; the surfaces of the ADC, entrance window, and filters are all tilted so that ghosts are minimised.
Largest Mirror	Largest working mirror is M4, 256×276mm; largest fold mirror is MF1 (i.e. in the common path), 260×380mm.
Tolerances	Are calculated for 70% strehl at 1μm. The tightest tolerances are 0.05mm and 0.01°, within manufacturable limits.
Intermediate Pupil	Beam is collimated at pupil; pupil shape varies with field position so cold stop must be undersized at 99.1mm. The fraction of light vignetted increases to 1.0% at the corner of the field.
Focal Plane	Focal plane is 261-266mm wide and 268-269mm high; it is tilted by 4.1° and is convex with a 1500mm radius of curvature (due to curvature from MAORY)
Image quality with SCAO	Strehl ratio exceeds 84% at 0.8μm (i.e. exceeds the limit defined for tolerancing) over the full 26"×26" field for SCAO.

3.2.3 Auxiliary Arm

The basic design of the auxiliary arm is shown in Figure 6.
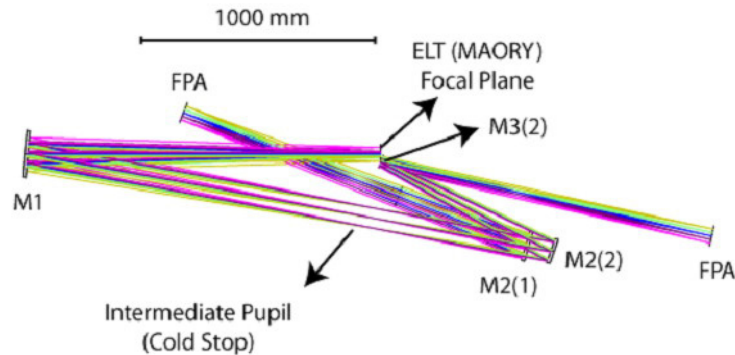
Figure 6: working mirrors for the auxiliary arm. M1 is the parabolic collimator; M2(1) re-images the focal plane at 4mas/pixel while M2(2) and M3(2) re-image it at 1.5mas/pixel. Additional flat fold mirrors ensure that the FPA is actually located in the same position in space for both pixel scales, i.e. only 1 detector is needed.

Table 2: characteristics of the optical design of the auxiliary arm

Throughput	60-69% for imaging in Y-K bands, 18-28% for spectroscopy in Iz-K bands
FoV & pixel scale	6.4"×6.4" at 1.5mas/pixel or 17.1"×17.1" at 4mas/pixel
Filters	Single filter wheel with 20 positions for filters and grisms

MICADO
Consortium

MICADO PHASE A

SYSTEM OVERVIEW

Doc: E-TRE-MCD-561-0009
Issue: 2.0
Date: 22.10.09
Page 11 of 30

Image Quality	Nominal strehl ratio over the whole field at 0.8μm is >89% for 1.5mas imaging; nominal strehl >75% in the longslit for the 4mas scale.
Distortion	-0.39% for the 4mas scale and 0.03% for the 1.5mas scale.
Ghosts	The reflective optics do not create ghosts; the surfaces of the ADC, entrance window, and filters are all tilted so that ghosts are minimised.
Largest Mirror	Largest working mirror is M1 (i.e. in the common path), 200mm diameter
Tolerances	Are calculated for 70% strehl at 1μm. The tightest tolerances are 0.05mm and 0.01°, within manufacturable limits.
Intermediate Pupil	Beam is collimated at pupil; pupil shape varies slightly with field position so cold stop must be undersized at 85.6mm. The fraction of light vignetted increases to 0.4% at the corner of the field.
Focal Plane	Focal plane is 61.4mm across and is unaffected by curvature from MAORY
Image quality with SCAO	Strehl ratio exceeds 78% at 0.8μm (i.e. exceeds the limit defined for tolerancing)

3.2.4 Optional Modes

There are a number of options that the consortium was requested to study, or which have been identified during the science analysis. These are mostly associated with the Auxiliary Arm. The conclusions about the optional modes are summarised in .

Table 3: summary of optional modes for MICADO

Optional Mode	Include?	Notes
Spectroscopy	Yes	Required by a number of science cases; R~3000 in order to probe between the OH lines; included in auxiliary arm
Changeable pixel scale	No	fixed pixel scale is preferred for primary arm, to maximise stability
	Yes	auxiliary arm has 1.5mas for imaging in extremely crowded fields and 4mas for spectroscopy
Coronagraphy	No	MCAO cannot provide the high Strehl ratio required for the PSF suppression at a level that would lead to high (i.e. scientifically interesting) dynamic range.
GLAO	No	Imaging with GLAO on the E-ELT is not competitive with JWST; a camera optimized for MCAO could in principle be used with GLAO, but it cannot simultaneously be optimized for GLAO (this would require a totally different camera

		design).
SCAO	Yes	The current concept is that MICADO should be used with SCAO at first light; and later be transferred to the MCAO system when it becomes available
Tunable Filter	TBC	The science cases identified this as a preferred option; there is strong interest from FRACTAL, Spain (Dr M. Garcia-Vargas) to explore this option for MICADO; see below.
High Time Resolution	TBC	NUI Galway, Ireland (Dr A. Shearer) have a strong track record of high time resolution astronomy and are interested in exploring this option for MICADO; see below.
OH suppressing filters	TBC	We have initiated a research and development project with Laser Zentrum Hannover to develop high throughput broad and narrow band filters, as well as OH suppressing filters. See RD5 for more details.

3.2.4.1   Tunable Filter

We are considering various options for a tunable filter that is able to image both line and continuum wavelengths simultaneously. One option, perhaps the most simple scheme, would be to use a standard Fabry-Perot etalon, but make use of the back-reflected light and image that on a second detector. The obvious disadvantage of this scheme is that an additional detector is required (although it could be smaller than $4k^2$ pixels). Another conceptually simple option would be to use a dichroic to split the light into 2 independent beams, each of which passes through a tunable FP. In this case it might be easier to image both beams on the same detector, but it is perhaps less desirable (although very much more flexible) to have 2 FPs; and each beam would lose a factor $\sqrt{2}$ in signal-to-noise. Another option would be to design a dual passband etalon or filter, for which the passbands are fixed relative to each other. If the filter was placed in a collimated beam and tilted in order to change the angle of incidence, the wavelengths of both passbands would change. After the filter, a prism could be used to separate the 2 images on the same detector. For such a system, one would need to carefully study the accuracy required, repeatability, number of dual passband filters needed, etc. This is work we plan to pursue during the Preparatory Phase, before Phase B begins.

3.2.4.2   High Time Resolution Detectors

Detector technology is available now in the range 0.8-1.2μm using APDs and pnCCDs [Hartmann et al. 06, Meidinger et al. 06, Hartmann et al. 08]. There is every expectation that electron multiplication systems will extend towards 2μm over the next two years. A high time resolution astronomy (HTRA) instrument is essentially a simple imaging device (small and cheap) with a fast detector. As such, an HTRA instrument suitable for inclusion within MICADO could be constructed today with a limited wavelength range (0.8-1.2μm) and within 2 years up to 2μm.

References:

Hartmann, Robert, Deires, Sebastian, Downing, Mark, Gorke, Hubert, Herrmann, Sven, Ihle, Sebastian, Kanbach, Gottfried, Papamastorakis, Janis, Soltau, Heike, Stefanescu, Alexander, and Strüder, Lothar, 2008, Proc. SPIE, 7015, Results of a pnCCD detector system for high-speed optical imaging

Meidinger, Norbert, Andritschke, Robert, Hartmann, Robert, Herrmann, Sven, Holl, Peter, Lutz, Gerhard, and Struumlder, Lothar, 2006, Nuclear Instruments and Methods in Physics Research A, 565, 257, pnCCD for photon detection from near-infrared to X-rays

Hartmann, Robert, Gorke, Hubert, Meidinger, Norbert, Soltau, Heike, and Struumlder, Lothar, 2006, Scientific Detectors for Astronomy 2005, A pnCCD Detector System for High Speed Optical Applications

3.3   Mechanics

The design of the mechanics, and folding of the optical path, has largely been driven by the limited space under MAORY. To keep torques small and to maintain optical alignment during cool-down, the centre of gravity is close to the optical axis which itself is close to the centre of shrinkage. In order to minimize cable lengths and to limit the mass mounted on the derotator, the electronics racks are mounted on a co-rotating platform supported on the Nasmyth floor. This platform also houses the cable-wrap for external supplies. Service and maintenance aspects are also key aspects of the design, leading to a design in which the core instrument and optics structure are rotated by 25° with respect to the cryostat. This provides better access through the cryostat doors to the detector arrays, the primary/auxiliary arm selection and focal plane mechanisms, the filter wheels, and the core optics.

3.3.1 Cryostat

MICADO is surrounded by a stainless steel cryostat as shown in Figure 7. This has a tapered fixed part which has sufficient space for all the through-ports and pumps. On either side are 2 large doors which provide access to all key components while MICADO is mounted to the AO system. Even when fully opened, the doors remain within the 3.8m diameter rotational volume of MICADO. The 2 electronics cabinets are positioned on the co-rotating floor-mounted platform in such a way that they do not interfere with the doors.

The entrance window of the cryostat is located 300mm above the focal plane and 200mm below the mounting interface. The warm ADC is located in this volume for the reasons outlined in Section 3.2.1. An intermediate support structure will house the ADC and also provide mechanical coupling between the top of the cryostat and the interface ring.
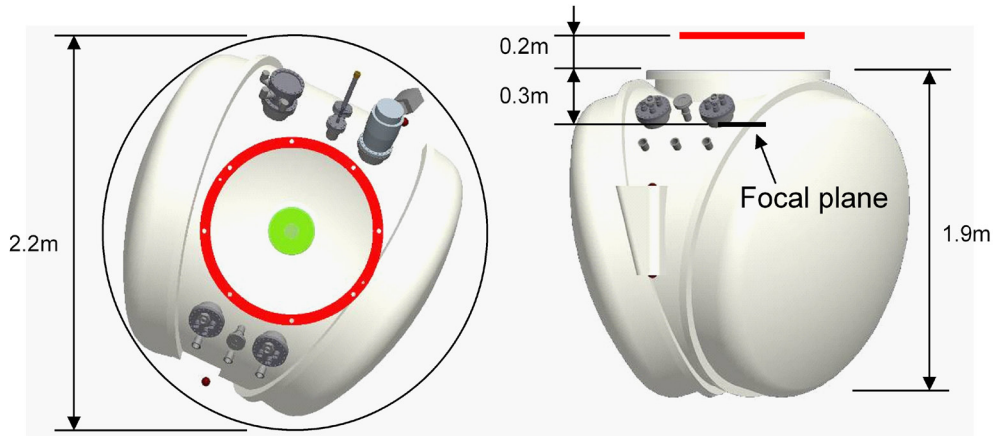
MICADO
Consortium

MICADO PHASE A

SYSTEM OVERVIEW

Doc: E-TRE-MCD-561-0009
Issue: 2.0
Date: 22.10.09
Page 14 of 30

Figure 7: Cryostat dimensions and relative position to MICADO mounting interface (red ring).

To minimise flexure (a critical issue for astrometry), the instrument has been designed for gravity invariant rotation. Because of this, and also because the cool-down times are limited by thermal contact of the filters, the cryostat has not been light-weighted. The mass estimates are given in Table 4

Table 4: mass and location of MICADO components

Location	Element	Mass estimate, tons
Below derotator	Cryostat	2.1
	Instrument	0.9
On Nasmyth Platform (rotating)	Rotating platform	1.2
	Electronics racks	1.1
	Cable wrap	0.5
In AO system (static, at input focal plane)	Calibration unit	0.5
	Total mass	6.3

3.3.2 Cold Optics Instrument

Within the cryostat and behind the radiation shield is the cold optics instrument, which is mechanically coupled to the cryostat. It comprises 3 main structures (see Figure 8): the primary arm, auxiliary arm, and core sub-assembly. The general design approach for each of these housings is to assemble them from plate material to keep part complexity and accuracy low, and ensure a rigid boxed structure. Stray light can be reduced by proper shielding and baffling, and also by using a wave-like finish to the surface of walls (as effectively used for SPIFFI and XShooter), and applying a low-reflectivity black coating. The filter wheels for each of the 2 arms are mounted on the side panels of the core structure, and supported at their perimeter. The primary and auxiliary arm housings are mounted to the core with a three-point interface in such

MICADO
Consortium

MICADO PHASE A

SYSTEM OVERVIEW

Doc: E-TRE-MCD-561-0009
Issue: 2.0
Date: 22.10.09
Page 15 of 30

a way that they connect to the round side panels with direct support underneath from the core wall panels.

The instrument core is supported by the cryostat via 3 V-rods and a transfer structure, also shown in Figure 8. The rods are co-axially aligned to maintain alignment during cool-down, and are attached to the transfer structure. This has been designed to accommodate the rotating focal plane mechanism, and acts as a bridge to the stiff support structure of the core sub-assembly.
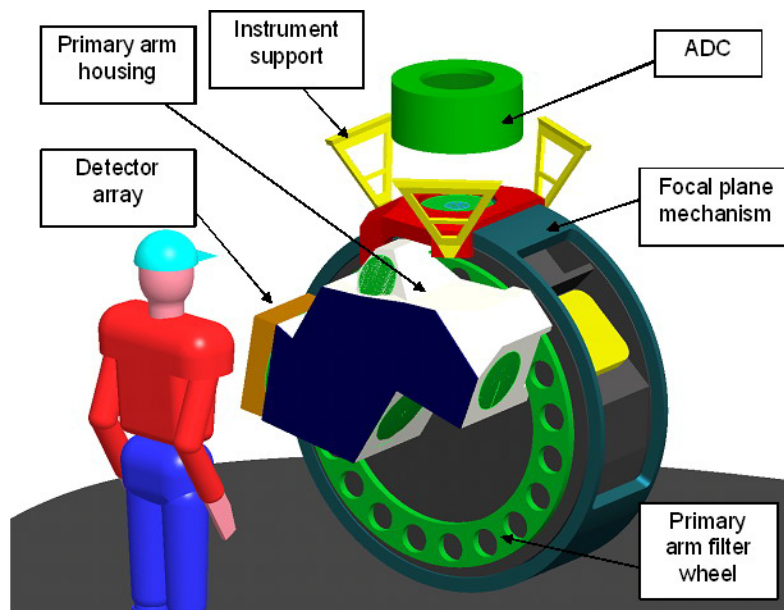

Figure 8: cold optics, comprising: primary arm, auxiliary arm (not visible), and the core sub-assembly. A filter wheel separates the core sub-assembly from each of the instrument arms, which are mounted to the core structure with 3-point connections. The core structure is mounted to the cryostat via the 3 V-rods (yellow) that are attached to the transfer structure (red), which itself is attached to the core sub-assembly. The focal plane mechanism (blue) rotates around the core sub-assembly and underneath the transfer structure.

3.3.3 Cold Mechanisms

MICADO has relatively few cold mechanisms:

Focal plane selection: the input focal plane is large, and 6 positions are required (field stop for each arm, 2 long slits, a closed position, and a point source mask for initial check of internal focus). It is a large structure that is driven around the outside of the core sub-assembly

Primary/Auxiliary Arm selection: the core contains only this one mechanism, which rotates in an alternative parabolic collimator mirror if the auxiliary arm is selected. Because this is recognised as being delicate, accessibility has been an important design driver, and is facilitated by a large opening in the focal plane wheel.

Filter wheels: The pupil sizes are 100mm and 86mm diameter for the primary and auxiliary arms. In order to provide space for 20 filter slots, these wheels are large, and hence supported

MICADO
Consortium

MICADO PHASE A

SYSTEM OVERVIEW

Doc: E-TRE-MCD-561-0009
Issue: 2.0
Date: 22.10.09
Page 16 of 30

and driven at their perimeter. Since the filters will dictate the cool-down time, care has been given to maximising the thermal contact.

Scale changing mechanism: the auxiliary arm has two mechanisms to move mirrors and enable a pixel scale change. The design is similar to the primary/auxiliary selection mechanism.

3.4 Cryogenics

A summary of the required temperatures and estimated heat loads is given in Figure 9. In order to avoid the use of cryo-coolers, the vibrations from which would have a strong adverse effect on the AO performance, MICADO will be cooled by continuous flow liquid nitrogen (LN2) during cool-down/warm-up cycles as well as steady state phases. For cooldown, an estimated 1000L will be needed; and to maintain steady-state the required flow rate is expected to be 63L/day.
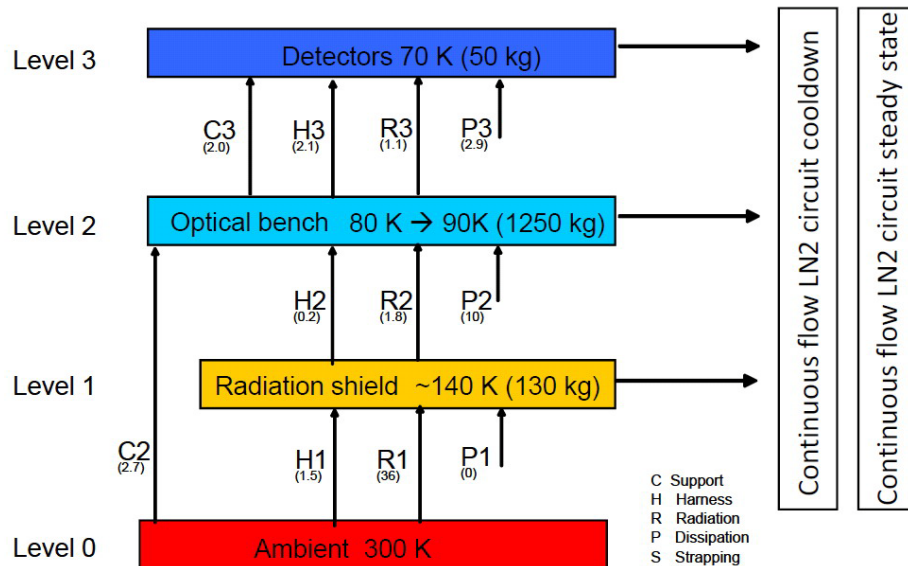

Figure 9: Overview of the temperatures and heat flows (given in brackets in units of Watts) for the different components within MICADO

The 3 modes of cryogenic operation are as follows:

Cool-down mode: flush with dry nitrogen – initial evacuation – cool down – stabilisation – sorption pump regeneration

Steady state (& failure) mode: continuous LN2 supply – defogging entrance window – emergency pumping if pressure and/or temperature rise – sorption pump regeneration

Warm-up mode: electric heater controlled warm-up with possible dry nitrogen warm-up – re-pressurisation with interlock via vacuum valve.

Continuous flow is preferred over a LN2 bath since it gives more freedom in the location of the detectors, it keeps the cryostat smaller and its mass lower, it is possible to combine the pre-cooling and steady state systems. Cooling pads are located at strategic points in the cryostat, and connected so that during a cool-down cycle the heat shield is cooled first, followed by the

MICADO
Consortium

MICADO P*HASE* A

S*YSTEM* O*VERVIEW*

Doc: E-TRE-MCD-561-0009
Issue: 2.0
Date: 22.10.09
Page 17 of 30

optical bench and finally the detectors. During steady state the sequence is reversed so that the detectors have the lowest possible temperature. This series concept is shown in Figure 10, which demonstrates how the same circuit can be used during both phases. Variations of this concept would allow the system to be closed so that LN2 can be pumped round the instrument multiple times, hence reducing the LN2 source flow required. The detectors will be partially thermally decoupled from the LN2 in order to damp out temperature fluctuations.
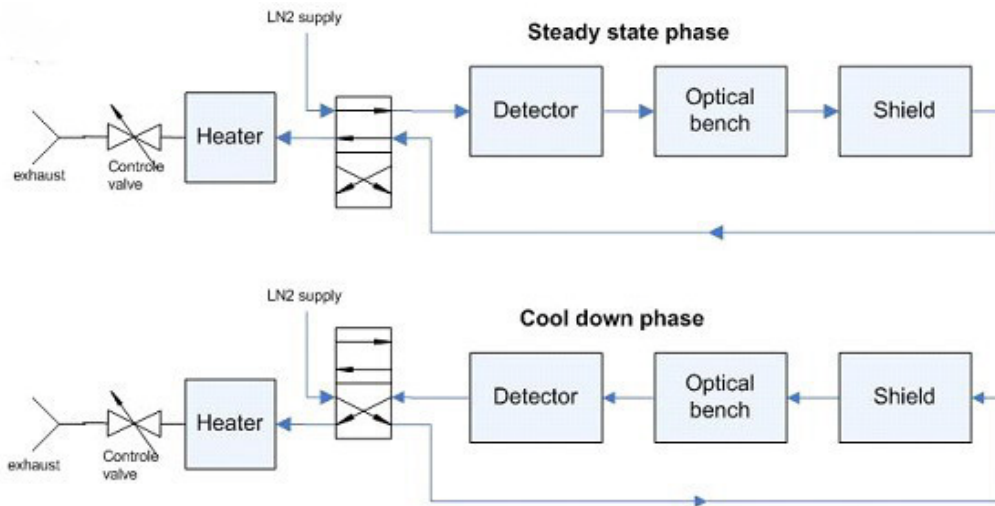

Figure 10: series cooling concept: for the cool-down phase, the heat shield is cooled first, then the optical bench and finally the detectors; during steady state the sequence is reversed to keep the detectors as cold as possible. In this concept, the same circuit can be used in both phases by reversing the direction flow.

3.5   Control Electronics

The preferences for MICADO include:

- Based on SIMATIC Programmable Logic Controller (PLC), Realtime Ethernet or other Realtime architectures

- Also for cryogenic housekeeping (cryogenics control) and safety relevant functions PLC SIMATIC S7 in fail safe version is a possible standard

- Realtime LabView and PXI controller from National Instruments could also be used as implementation for control electronic

3.6   Instrument Software

The user requirements for the instrument software have been developed for observation preparation, science operations (including on-sky calibration), and maintenance operations. The main functionality has been analysed via specific use cases related to the various observing

MICADO
Consortium

MICADO PHASE A

SYSTEM OVERVIEW

Doc: E-TRE-MCD-561-0009
Issue: 2.0
Date: 22.10.09
Page 18 of 30

scenarios and modes. An overview of the complete scheme is given in Figure 11. Specific use cases include:

Perform Science Observation: science imaging, science spectroscopy, photometric/atmospheric standard stars, measure twilight flats, etc.

Perform Calibration: Measure dark frames, measure internal flatfield, measure linearity, calibrate wavelength, assess ghosting, measure distortion.

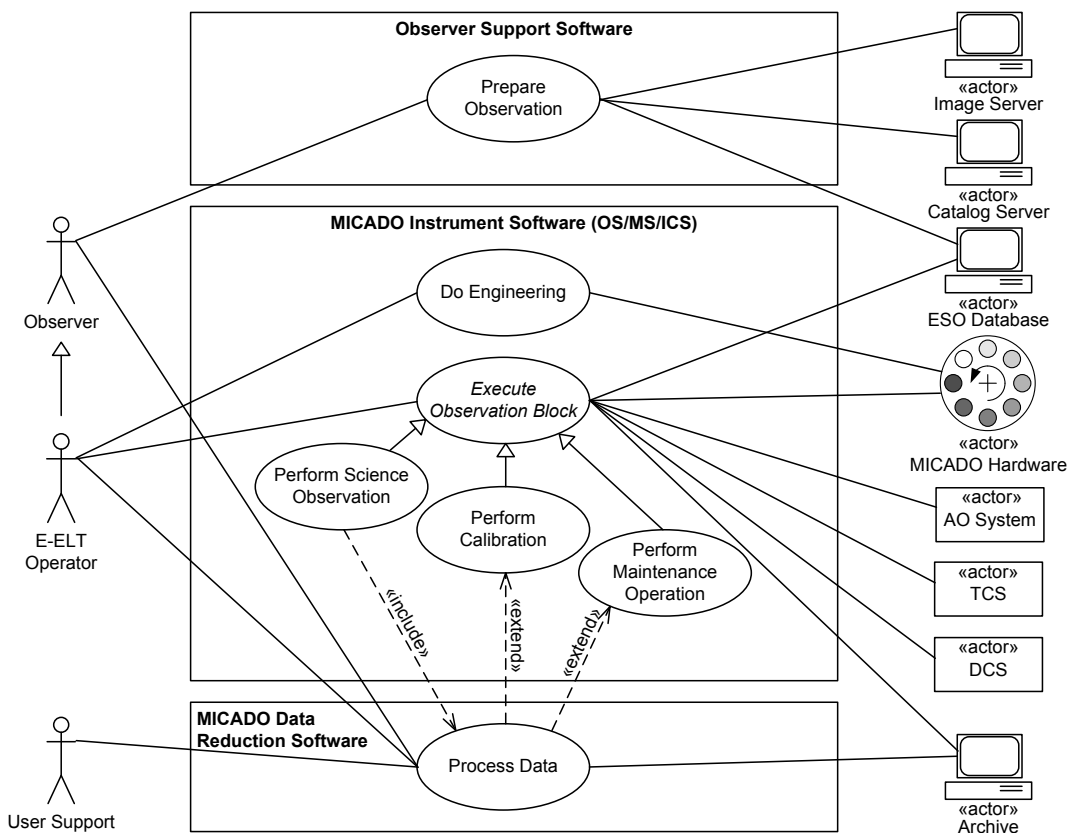*Perform Maintenance Operation*: determine telescope focus.

Figure 11: Global scheme for the MICADO instrument software, together with all external actors (personnel, databases, hardware, control systems, etc).

The preferences for MICADO regarding possible software platforms and programming languages are:

1. Given the timeline of the project it will be necessary to maintain a certain development infrastructure (possibly including licenses for operating systems and/or software development kits) for many years. Therefore Open Source solutions are strongly preferred over proprietary commercial ones. For the same reason Linux as operating system will be favoured.

2. Because of good experiences with C++, Python and XML these could be imagined as a suitable set of standard programming languages.

MICADO
Consortium

MICADO PHASE A

SYSTEM OVERVIEW

Doc: E-TRE-MCD-561-0009
Issue: 2.0
Date: 22.10.09
Page 19 of 30

3.7 Data Reduction

The user requirements for the data reduction software have been developed from the observational scenarios for imaging and spectroscopy. These are standard, well understood, techniques, and lead to no surprises. The performance required for photometry and astrometry have lead to additional requirements. These include the use of a special internal calibration mask to measure instrument distortions, and additional steps in the data processing for the related science projects.

The Astro-WISE system is well suited for reduction of MICADO data. Astro-WISE is an integrated system where users cannot only perform data reduction but also data archiving, post-reduction analysis and publishing of the raw, intermediate and final data products.

A salient feature for the data reduction relevant for MICADO is that it performs 'global' astrometry and photometry. Astrometric and photometric corrections and calibrations by combining the information from overlapping observations improving on calibrations based on individual pointings. Data reduction can take place in fully automated fashion or in a more manual fine-tuning manner.

The data rates estimated for MICADO are up to about 6Terabytes per night (if all individual exposures are kept and processed for optimal astrometric accuracy); although significantly less if either short exposures can be directly co-added in the DCS, or longer exposures are required (e.g. when using narrow band filters).

3.8 Single Conjugate Adaptive Optics Module

3.8.1 Rationale for a SCAO module

The MICADO design to achieve superb sensitivity and resolution, enable precise astrometry, and provide high throughput spectroscopy, is simple, compact, and robust. This minimizes risk of both cost and schedule. As a result, the consortium has identified a phased approach as an important option. Thus, while MICADO achieves superb wide-field performance with the MCAO module MAORY, in its first phase MICADO will be combined with an internal SCAO module. As this simple on-axis, natural guide star mode sets low requirements on the telescope and AO performance (no lasers), MICADO+SCAO is thus an optimum choice for demonstrating the scientific capabilities of the E-ELT at first light.

3.8.2 Top Level Requirements

The SCAO module was not part of the original call for proposals. When it was included in the MICADO design study following the mid-term review, its top-level requirements were established with the goal to address similar science goals as for MAORY (although with restricted target choice, etc). While developing the TLR, it was borne in mind that the SCAO module is expected to be used only during the first few years of MICADO operations and could consequently work with restricted specifications (e.g. field of view). And it was decided to adopt, as far as possible, the same interfaces that MICADO has with MAORY.

MICADO
Consortium

MICADO PHASE A

SYSTEM OVERVIEW

Doc: E-TRE-MCD-561-0009
Issue: 2.0
Date: 22.10.09
Page 20 of 30

Table 5: summary of the MICADO SCAO module Top Level Requirements

TLR #	description	value	comment	fulfilled
SCAO_TLR1	Patrol field of view	45"	Diameter	Yes
SCAO_TLR2	WFS bandpass	0.45-0.8μm		Yes
SCAO_TLR3	Repositioning accuracy for small dither	2 mas	Offset value: ±0.3 arcsec Offset timescale: few tenths of second (TBC) AO loop closed between offsetting The offset is done by AO	Yes
SCAO_TLR4	Repositioning accuracy for large dither	2 mas	Offset value: few seconds Offset timescale: up to 30 sec (TBC) AO loop closed on both offset positions, opened during offsetting The offset is done by the telescope	Yes
SCAO_TLR5	Relay optics image quality	80% @ 0.8μm		Yes
SCAO_TLR6	Relay optics magnification	1	As for MAORY	Yes
SCAO_TLR7	SCAO module transmission	80%	At infrared wavelengths	Yes
SCAO_TLR8	SCAO module above MICADO, in a gravity invariant position			Yes

3.8.3 SAMI: SCAO for MICADO

SAMI is the Single Conjugate Adaptive Optics module for MICADO. It can be seen in Figure 3 and is composed of 5 sub-systems:

- an optical relay made of a 3-mirror Offner relay, a folding mirror directing the light downward to MICADO and the WFS, and a dichroic plate splitting the light between MICADO and the WFS.
- a field derotator to compensate for the telescope movements while tracking, for both MICADO and the WFS.
- a structure supporting the whole assembly, i.e. the optical bench of the relay optics, the WFS, the derotator and MICADO.
- a pick-off mirror with tip-tilt capabilities to correct for the pupil issues and WFS misalignments (but not for atmospheric tip-tilt),
- the WFS made of a field stop, a K-mirror for pupil derotation, a lens triplet and the WFS camera. All are mounted on XY stages to pick up the reference source light in the field and ensure jitter/offset capabilities.

The initial study, to be refined and confirmed, has shown that an ADC in the WFS should not be necessary.

The mass of the SCAO module and its support structure is given in Table 6.

MICADO
Consortium

MICADO PHASE A

SYSTEM OVERVIEW

Doc: E-TRE-MCD-561-0009
Issue: 2.0
Date: 22.10.09
Page 21 of 30

Table 6: mass estimate for SCAO module and its support structure

item	*Mass (kg)*
Mounting structure	2000
Optical relay	1470
Derotator	610
WFS	170
Total	**4250**

3.8.4 Real Time Computer

The control law we plan to implement is a classical integrator, with a modal control, together with a Kalman filtering for the windshake compensation. We also plan to use smart algorithms for the centre of gravity computation such as the weighted centre of gravity method or centroiding by pixel selection.

3.8.5 Performance

The performance of the MICADO SCAO module has been estimated using analytical formulae (e.g. for the anisoplanatism error), information from ESO (e.g. for the fitting error) and two home-made simulation tools. The results are summarized in Table 7 and Table 8.

Table 7: summary of anisoplanatic effect on strehl ratio for SCAO

Distance from reference source (arcsec)	5	15	25	35	45	55
Anisoplanatism error for L_0=25m (nm rms)	101	253	354	433	518	554
Corresponding Strehl ratio scaling at 2.2 μm	92%	59%	36%	22%	11%	8%

Table 8: summary of SCAO performance as a function of guide star magnitude

On-axis reference source magnitude	m_V=12	m_V=13	m_V=14	m_V=15	m_V=16
Total error (nm rms)	183	205	245	328	514
Strehl at 2.2 μm	76%	71%	61%	41%	12%

MICADO
Consortium

MICADO PHASE A

SYSTEM OVERVIEW

Doc: E-TRE-MCD-561-0009
Issue: 2.0
Date: 22.10.09
Page 22 of 30

4 OPERATIONAL CONCEPT & CALIBRATION

4.1 Preliminaries

The fundamental goal of MICADO's operational concept is to maximize the scientific return of the instrument. In terms of observing strategy, this relates directly to the reduction of noise.

Figure 13 illustrates the various sources of noise associated with near-infrared ground-based astronomical observations. Noise falls into two broad categories: those associated with natural phenomena, such as the intrinsic brightness of the science target and sky; and those which arise within the instrument. The opto-mechanical and electronic design of MICADO itself addresses the latter category, and the reader is referred to RD5 for further details on the reduction of excess thermal background from the instrument.
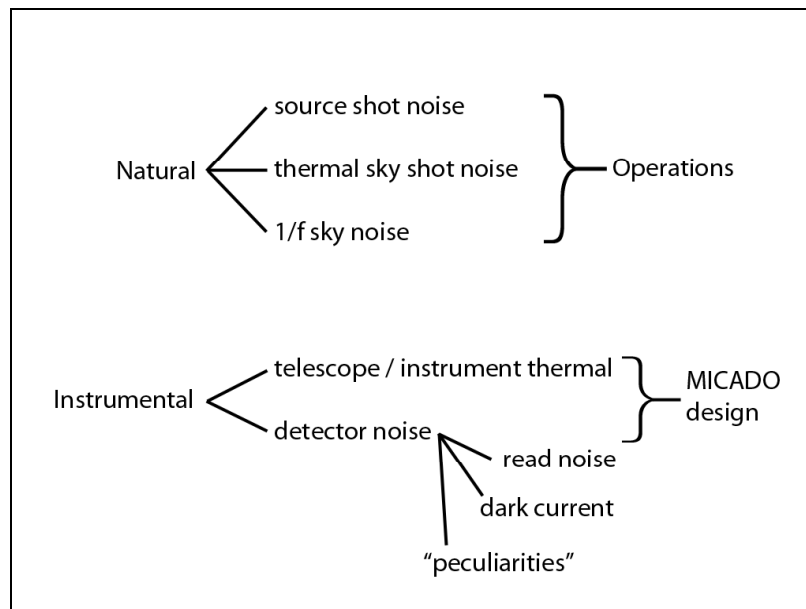

Figure 12: Noise sources associated with near-infrared ground-based astronomy. The detector "peculiarities" include FET glow, recombination noise in photoconductors, shading, persistence, etc. Proper operations can address the natural sources of noise, while proper opto-mechanical and electronic design is the most important remedy for instrumental noise.

Proper operation can address the "natural" noise sources. For example, shortening the exposure time, or in extreme cases introducing a neutral density filter, can reduce the Poisson shot noise from the source. We are very rarely in the situation when our sources are too bright, however, and essentially all astronomers would be delighted to have their observations be source-noise limited. In fact, for near-infrared, ground-based astronomy with a well-designed instrument, thermal and 1/f sky noise dominate. Proper operation of MICADO can minimize these noise sources.

MICADO
Consortium

MICADO PHASE A

SYSTEM OVERVIEW

Doc: E-TRE-MCD-561-0009
Issue: 2.0
Date: 22.10.09
Page 23 of 30

4.1.1 Sky Noise and Signal-to-Noise Ratio

For a given near-infrared observation, the Signal to Noise Ratio (SNR) is:

$$SNR = \frac{G \cdot F_o \cdot t}{\sqrt{N_{pix} \cdot \left[(G \cdot F_{tot} + I_d) \cdot t + RN^2 \right]}}$$

where G is the gain of the detector, F_0 is the total flux from the object, t is the integration time, N_{pix} is the number of pixels illuminated by the object, F_{tot} is the total flux per pixel from all sources, I_d is the dark current, and RN is the read noise.

Only the read noise term in this equation is independent of time. In other words, a single observation will take a single read noise penalty, while the contributions from the source shot noise, sky, telescope, and instrument background (F_{tot} and I_d in the denominator) increase with time. With typical modern detectors and observing conditions, this has the consequence that the SNR increases linearly with exposure time while the fixed read noise term dominates, then turns over to a slower, square-root, increase as the thermal background term takes over (modern detectors have negligible dark current for typical observations). Figure 14 shows the increase of SNR with exposure time.
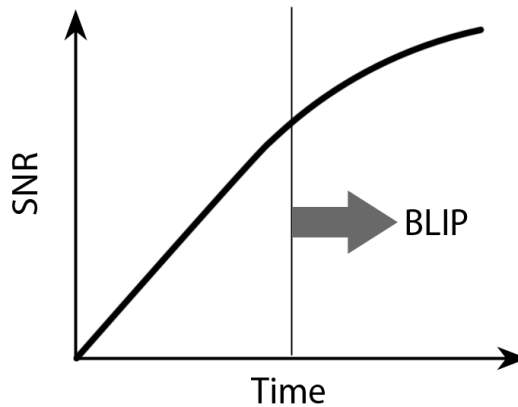

Figure 13: The increase in Signal to Noise Ratio with increasing exposure time. The turnover point between linear and square-root behaviour denotes background-limited performance.

The bend in the curve in Figure 14 occurs approximately when the two terms under the square-root are equal – in other words, when the total accumulated background flux equals the square of the read noise. This situation is known as the *background limit*, and an instrument operating to the right of this point is providing *background-limited performance*, or *BLIP*. Integrating for much longer than the time needed to reach the background limit does not provide any advantage to the observer, since a series of independent exposures will also increase the S/N ratio as the square root of time. In fact, the variability of the sky level (see below) and other factors, such as cosmic rays and electronic glitches, make it advantageous to end an exposure when the background limit is reached.

For MICADO, which is planned to make use of HAWAII-4RG detectors, AD5 indicates that a short exposure will have ~25 electronics read-noise. In the H-band, we expect approximately

MICADO
Consortium

MICADO PHASE A

SYSTEM OVERVIEW

Doc: E-TRE-MCD-561-0009
Issue: 2.0
Date: 22.10.09
Page 24 of 30

33 electrons per second per pixel of background, overwhelmingly from the sky (see Section 6). Therefore, broad-band H observations will reach BLIP in approximately 20 seconds (although with continuous non-destructive reads, each of 0.665sec (AD5), in this time the read-noise would have been reduced by a factor ~4 and so one would be well beyond the BLIP limit). We note, however, that on-going improvements in detector technology are likely to drastically reduce the single read noise of the detectors. Indeed, improved pond pad resistance already means that the KMOS detectors have a single read noise below 10e- , in comparison to the XShooter detectors which had 25e- noise (G. Finger, priv. comm.). In such a case, one would reach BLIP in only ~3 seconds. Of course, the transition from read-noise to background-limited measurements is not instantaneous, and experienced observers typically go a few times beyond the BLIP limit – say 5 or 10 seconds per exposure in the example described.

Note that we have ignored the photon shot noise associated with the target source in the discussion above, since the sky is usually considerably brighter than the object. In those lucky instances when the target is considerably brighter than the sky, the observer can achieve good signal to noise ratio very quickly, and the observing efficiency is then limited by telescope moves, exposure setup, etc.

A different limit on exposure times may be imposed by the finite well depth of 45ke- (AD5). This implies that sources of H_{AB}=15.6 mag will saturate in the shortest DIT. Thus the exposure time will depend on the magnitude at which the observer wishes to avoid saturating, but the implication is that individual exposure times will typically be only a few seconds. It should nevertheless be noted that if there are bright targets in the field, one option is to use a narrow band filter; another is to operate the detector at a 100× faster pixel rate (up to 10Mpix/sec/output (R. Blank, priv. comm.), although at the expense of noise). An alternative that could be explored further is the option of hybrid readout modes, in which defined subsections or even specific pixels of an array are readout fast while most of the array is readout at a normal speed. Such functionality is already available (R. Blank, priv. comm.), and could provide the best solution to the saturation problem.

4.1.2 1/f Sky Noise and Nodding

The other important source of sky noise is so-called "1/f" noise. This arises due to fluctuations in atmospheric transmission, and hence the emissivity. This, in turn, produces variations in the thermal background flux. Water vapour is often the culprit, particularly at longer wavelengths. In otherwise excellent conditions, 1/f noise can be particularly troublesome, since a small change in background can have a relatively large effect.

The sky background variations have a 1/f temporal character (hence the name). This means that regular sampling of the sky by nodding the telescope is essential for successful observations. A naive assessment of the 1/f behaviour would require infinitely rapid sky sampling, but of course, operational overheads such as reading the detector, moving the telescope, etc., shift the optimum sky-sampling rate to considerably lower frequencies. Needless to say, the desire to operate in the background limit (see Section 5.1.1) also has an important influence on the cadence of observation and sky sampling.

MICADO
Consortium

MICADO PHASE A

SYSTEM OVERVIEW

Doc: E-TRE-MCD-561-0009
Issue: 2.0
Date: 22.10.09
Page 25 of 30

4.1.3 Sky Sampling and Adaptive Optics

Efficient operation of the MICADO instrument will require careful coordination of the camera with the facility adaptive optics, either MAORY or the SCAO system. As described in the previous sections, near infrared observations require regular sampling of the sky, in order to remove background variations and reduce $1/f$ sky noise. This is usually accomplished by nodding the telescope a small distance on the sky after taking an exposure and taking a subsequent frame, which is subtracted from the object frame.

Nodding of the E-ELT to reach an adjacent sky region will have operational consequences for the adaptive optics system. Specifically, natural guide stars used to maintain tip and tilt will move. Any such nodding will have to be choreographed between the AO and camera systems.

4.1.4 How Far? How Frequent?

The anticipated size and frequency of sky offsets depend critically on the particular science program. In the best instance, in which the target sources are point-like and well dispersed on the sky, offsets of only a few times of the PSF diameter should suffice. For extended sources, however, very significant offsets, perhaps involving re-acquisition of the tip tilt star, may be required.

As shown in Table 11, broadband observations with MICADO may require sky sampling with a cadence of 30 seconds to a few minutes. This pattern must be maintained throughout the observing session, resulting in several hundred telescope offsets per night. However, because of the large overheads that can accrue from large offsets, a modified offsetting scheme – an attempt at an optimal compromise between science requirements and practical issues – has been developed together with the MAORY consortium. This is summarised in Table 12.

Table 9: Science-driven magnitude and frequency of offsets needed to minimize sky background and 1/f noise.

	Good Conditions	Poor Conditions
	Shorter λ or Narrow Band Filters	Longer λ or Broad Band Filters
Point sources	2-3" offsets cadence: minutes	2-3" offsets cadence: 30-120 sec
Extended sources or fields with many distributed sources	10-20" offsets cadence: minutes	10-20" offsets cadence: 30-120 sec

MICADO
Consortium

MICADO PHASE A

SYSTEM OVERVIEW

Doc: E-TRE-MCD-561-0009
Issue: 2.0
Date: 22.10.09
Page 26 of 30

Table 10: AO- and telescope- driven magnitude and frequency of offsets (to reduce overheads)

Small dither	Offset of up to ±0.3" (goal ±0.5") from the initial pointing in each of X- and Y-directions, with an accuracy of <2mas. AO loops remain closed.
	Cadence: 10-30sec
Large dither	Offset of up to ±10" from the initial pointing. AO loops open during the offset and telescope is involved.
	Cadence: a few minutes
Sky Offset	Offset of up to 15' (when background cannot be recovered by dithering). AO loops do not need to close in the offset position; telescope may need to preset to reach required offset, and it is likely that pupil quality should be maintained and that the telescope GLAO loops should be closed.
	Note: sky offsets of 'up to 60arcsec' as per the Observatory TLR make no sense in the context of MICADO, which has a 53" field of view.
	Cadence: 20-30 minutes (depends on overhead)

4.2 Operational Concept

The foregoing considerations must be included in the operational concept for MICADO. The following scenarios address target acquisition and observing sequences for the primary imaging and auxiliary arms of the instrument. The specific instances of these more general scenarios and considerations have been detailed and developed in the Top Level Instrument Software User Requirements (RD7).

4.2.1 Acquisition of the Primary Imaging Field

Since the field of view is ~53 arcsec, in most cases highly accurate centering will not be required. It is therefore expected that, following a preset, there will typically be no additional offset. However, the option for accurate centering is foreseen (e.g. to put a bright star in a gap between detectors). Therefore, once the AO loops are closed, acquisition can include a number of large and/or small dithers (as described above) if required by the observer.

4.2.2 Observing with the Primary Imaging Field

4.2.2.1 Exposure times

We anticipate up to approximately 140 photo-electrons per pixel per second from the telescope, AO system, and sky background in the K band. With narrowband filters operating in the J and H photometric bands, however, the background level may be considerably less than one photo-electron per second. Ideally, the camera should be read out once the observations have reached a few times the background limit (see previous section).

For the detectors planned for MICADO, observations will reach the background limit at a few 10s of electrons. Thus, we anticipate exposure times ranging from a few seconds to a few minutes, depending on the filter in use. For exposure times of only a few seconds, multiple exposures will be made at the same pointing.

MICADO
Consortium

MICADO PHASE A

SYSTEM OVERVIEW

Doc: E-TRE-MCD-561-0009
Issue: 2.0
Date: 22.10.09
Page 27 of 30

4.2.2.2 Dithering

The dithering sequence outlined below has been developed based on the various dither and offsett options given in Table 12.

We note that the small and large gaps between the detectors are expected to be 3mm and 9mm respectively, corresponding to 0.6 and 1.8arcsec. Large dithers of at least 1.8arcsec in both directions will be needed to ensure that no region continuously falls into a gap during a sequence of observations.

The galaxy evolution science case has a requirement for 10 arcsec dithers every 1-2 minutes in order to enable optimal background subtraction and flat-fielding. This requirement applies equally to most science cases. The Galactic Centre science case imposes an additional requirement of dithering to a sky field, the nearest of which is 15 arcmin away.

A typical observing sequence for broadband K would then go as follows: pointing at the target and taking 3-10 short (few second) exposures, followed by a small dither (i.e. one that can be performed without opening the AO loops, and with only a small overhead). This sub-sequence would then be repeated 3-10 times and be followed by a large dither. During a 1 hr observing block, the complete nested sequence could be repeated up to 14 times (allowing for a 5min preset).

In cases where a sky offset is required (e.g. any crowded field, such as the Galactic Center, globular clusters, or nearby galaxies), it is foreseen that this would typically be performed only once, or at most twice, during such a sequence to maintain an acceptable efficiency.

For the narrowband case, there would be very few (or even just one) exposures per small dither, but otherwise the sequencing would be very similar.

4.2.3 Acquisition with the Auxiliary Arm

The field of view of the auxiliary arm is small: 6" for the 1.5mas pixel-scale imaging mode. This, coupled with the desire to perform long slit spectroscopy with this arm using a slit ~12mas wide (and a 4mas pixel scale), sets strong requirements on telescope centering. As a result, an acquisition is expected to require a large and then a small offset iteration in order to center the science target sufficiently well following a preset and closing of the AO loops.

This can be done either using the science target itself, if it is bright enough; or using a reference target within the field of view. In the latter case, the exact offset between the reference and science targets must be known (e.g. from pre-imaging), and the reference target is centered so that the location of the science object is on the required pixel. The concept for spectroscopy is that the target or reference should be accurately positioned while imaging at the appropriate scale; and only after the acquisition has been performed should the slit mask be moved in.

4.2.4 Observing with the Auxiliary Arm

4.2.4.1 Exposure Times

The Auxiliary Arm will be used mostly for narrow-band imaging (perhaps even the extreme case of imaging through a Fabry-Perot interferometer), spectroscopy, etc. These techniques require longer integration times, leading to typical individual exposure times of 1-2 minutes.

MICADO
Consortium

MICADO PHASE A

SYSTEM OVERVIEW

Doc: E-TRE-MCD-561-0009
Issue: 2.0
Date: 22.10.09
Page 28 of 30

There should be minimal positional drift on these timescales.

4.2.4.2 Dithering

For imaging with a small field of view, relatively small dithers (~0.1 arcsec), as well as offsets to sky (a few arcsec up to 15 arcmin) will be required. The observing sequence is the same as for the primary imaging field.

For spectroscopy, we foresee nodding up and down the slit. Ideally, the nod length would be a significant fraction of the slit. However, the spectroscopic mode implemented is optimised for compact targets, and so much smaller nod lengths may be acceptable. In the current concept, we foresee using small dithers to nod along the slit. This will enable us to maintain an accurate centering of the science target perpendicular to the slit. By setting the first nod positions at opposite extremes with respect to the initial pointing, the nod length can be as much as 0.6" (with a goal of 1.0").

For extended sources (e.g. the nuclei of nearby galaxies), it will be necessary to offset to sky. The method for doing this is the same as with the primary field, although if the sky offset is less than the 60" maximum defined in the Observatory Top Level Requirements, no time-consuming additional presets will be necessary.

4.3 Calibration

MICADO's photometric and astrometric performance will depend on careful calibration. Inevitably, there will be the usual suite of internal calibration sources, such as an integrating sphere for photometry (flatfields) and discharge tubes for spectroscopic work (wavelength calibration). These calibrations are considered standard and can be performed during daytime, unless there is a specific requirement from an OB to perform them during the night immediately after the science observations.

High precision astrometry will require special calibrations using additional hardware. For example, an accurate Hartmann screen placed in the camera focal plane would allow long term monitoring and calibration of the pixel scale and field distortions. This is particularly important since there will inevitably be discontinuities between the detectors in the MICADO focal plane (both translational and rotational), and because the MAORY field distortions will rotate with respect to those of MICADO. These calibrations can also be performed during daytime, and will require making many measurements with the rotator set at various angles.

All the above calibration sources will be located inside a dedicated calibration unit, which will be mounted in front of the AO system at the input focal plane. This is particularly necessary for the distortion calibration, which must be done here because (i) the focal plane is very nearly flat, and (ii) it is then possible to calibrate the MAORY distortions.

We anticipate that these daytime calibrations can all be completed either totally internal to MICADO under observatory daytime conditions or during the "dark" period allotted to instruments during an EELT operational day.

A few on-sky calibrations will be needed in addition to the internal calibrations. To compensate for vignetting and non-uniformity of the flatfield illumination, twilight flats will be needed.

MICADO
Consortium

MICADO PHASE A

SYSTEM OVERVIEW

Doc: E-TRE-MCD-561-0009
Issue: 2.0
Date: 22.10.09
Page 29 of 30

Table 13 summarises the calibrations required for MICADO, together with the frequency with which they will need to be taken, and whether they should be done during day-time or night-time. These have been derived from RD8. We note that some calibrations are bandpass dependent (e.g. flatfields, standard stars). Since MICADO has a baseline of 20 filters for the primary arm and 20 filters for the auxiliary arm, this could be rather time consuming. Instead, these only need be done on an 'as needed' basis, for example to match the bandpasses used for recent science data.

Table 11: Summary of calibrations required for MICADO and the frequency with which they should be done

calibration	*night/day*	*frequency*	*notes*
Bias (internal)	day	1 per day	For health checks only; basically a dark with minimum exposure time
Darks (internal)	day	1 per day	One of the focal plane masks will completely block the light (this could alternatively be done with a blanked-off filter slot)
Flatfield (internal)	day	1 per day	For pixel-to-pixel gains; source does not need to be spatially uniform
Flatfield & illumination correction (sky)	twilight (IJHK) or night (HK)	1 per month	may be possible to use (sparsely populated) science data for H & K bands since background is high.
Flux (standard star)	night	1 per night	Single standard star for flux calibration
Instrument distortions (internal calibration mask)	day	1 per 3 months	Need to have MAORY & MICADO at different rotations to create a full look-up table; this can also be used to generate PSFs for calibrating non-common path errors.
Electronic Ghosts	day	1 per month	Use same internal calibration mask also to assess ghosting, for removal by post-processing
Arclamps (internal)	day	1 per night	
Focus (star on sky)	twilight	1 only (TBC)	to set focus of MAORY & MICADO
linearity	day	1 per month	Internal flatfields of increasing integration times

MICADO
Consortium

MICADO PHASE A

SYSTEM OVERVIEW

Doc: E-TRE-MCD-561-0009
Issue: 2.0
Date: 22.10.09
Page 30 of 30

5 APPENDIX:

5.1 Throughput, Emissivity, and Thermal Background Calculation

The operational strategies presented in Section 5 were based on an assessment of the various thermal background sources present during MICADO observations. The following pages present the calculation of these in detail, starting with the throughput and emissivity, and using these to derive the background for each of the J, H, and K bands.

The 'bottom line' is that the emissivity of MICADO is dominated by the warm ADC and entrance window and is ~13% of the telescope background in each of these broad bands, close to the specification of 10%. However, we note that the telescope contributes only a part of the background. The relative contributions within each of these bands, assuming an ambient temperature of 10°C, are given in Table 14.

Table 12: relative contributions to total thermal background at 10°C ambient temperature

	J	H	K
Sky	100%	99%	38%
Telescope	0%	<1%	28%
MAORY	0%	<1%	29%
MICADO (warm+cold)	0%	<0.1%	4%

---oooOOOooo---

This document calculates the system transmission for MICADO on E-ELT

The optical system contains warm and cold mirrors and glass Those that are warm can be clean or dirty, which effects transmission. We assume 5% increased emissivity for dirty aluminum.

We assume the folllowing composition of the optical systems:

E-ELT - 6 warm reflection, 4 clean and 2 dirty (M1, M3)
MAORY - 8 warm clean reflections and 1 glass element (vis-IR dichroic)
MICADO - ADC+window = 4+1 warm glass elements, 8 cold clean reflections, filter, detector

Throughput of individual components

$Rg := 0.99$ 　　　　　　　　　　　　　　Reflectivity of Gold (unused)

$Ra_0 := 0.96$ 　　$Ra_1 := 0.97$ 　　$Ra_2 := 0.975$ 　　CLEAN Aluminum at J,H,K

$Rd_0 := 0.91$ 　　$Rd_1 := 0.92$ 　　$Rd_2 := 0.925$ 　　5% DIRTY Aluminum at J,H,K

$QE_0 := 0.95$ 　　$QE_1 := 0.95$ 　　$QE_2 := 0.92$ 　　Detector QE at J,H,K (ESO figures)

$Tg := 0.99 \cdot 0.99 \cdot 0.995$ 　　　$Tg = 0.975$ 　　Transmission of glass element (lens, window, etc. - 2 AR coatings + bulk)

$T\varepsilon g := 0.995$ 　　　　　　　　　　Glass bulk absorption only for ε

$Tf := 0.8$ 　　$Tatm := 0.95$ 　　　　　Transmission of filters, atmosphere

Calculate for J, H, K bands... 　　$j := 0..2$ 　　$\lambda_0 := 1.25$ 　$\lambda_1 := 1.65$ 　$\lambda_2 := 2.2$

$Ttel_j := \left(Rd_j\right)^2 \cdot \left(Ra_j\right)^4$ 　　　　Dirty primary and tertiary - the rest are clean

$Tma_j := \left(Ra_j\right)^8 \cdot Tg$ 　　　　　MAORY is 8 clean reflections + dichroic

$Tmic_j := (Tg)^5 \cdot \left(Ra_j\right)^8 \cdot Tf \cdot QE_j$ 　　MICADO is ADC (4 glasses), window, 8 cold clean mirrors, filter, detector

Subsystem Transmission 　　$Ttel = \begin{pmatrix} 0.703 \\ 0.749 \\ 0.773 \end{pmatrix}$ 　　$Tma = \begin{pmatrix} 0.703 \\ 0.764 \\ 0.796 \end{pmatrix}$ 　　$Tmic = \begin{pmatrix} 0.484 \\ 0.525 \\ 0.53 \end{pmatrix}$

Total Optical Throughput 　　$Ttot_j := Tatm \cdot Ttel_j \cdot Tma_j \cdot Tmic_j$ 　　$Ttot = \begin{pmatrix} 0.227 \\ 0.286 \\ 0.31 \end{pmatrix}$

We now calculate the relevant warm and cold emissivities. This is just 1-T, where T is the throughput.Note that we include only the bulk absorption of the glass elements, since the surface reflections either return to the sky or to the cold cryostat.

WARM Emissivities

$$\varepsilon Wtel := 1 - Ttel \qquad \varepsilon Wma := 1 - Tma \cdot \frac{T\varepsilon g}{Tg} \qquad \varepsilon Wmi := 1 - (T\varepsilon g)^5$$

$$\varepsilon Wtel = \begin{pmatrix} 0.297 \\ 0.251 \\ 0.227 \end{pmatrix} \qquad \varepsilon Wma = \begin{pmatrix} 0.282 \\ 0.22 \\ 0.187 \end{pmatrix} \qquad \varepsilon Wmi = 0.025$$

Total

$$\varepsilon W_j := 1 - \left(1 - \varepsilon Wtel_j\right) \cdot \left(1 - \varepsilon Wma_j\right) \cdot (1 - \varepsilon Wmi) \qquad \varepsilon W = \begin{pmatrix} 0.508 \\ 0.43 \\ 0.387 \end{pmatrix}$$

COLD Emissivities (this is just MICADO)

COLD Throughput (for emissivity)
$$Tcold_j := \left(Ra_j\right)^8 \cdot Tf$$

This is the 8 cold reflections
and 1 filter within MICADO

$$\varepsilon C := 1 - Tcold \qquad \varepsilon C = \begin{pmatrix} 0.423 \\ 0.373 \\ 0.347 \end{pmatrix}$$

This document calculates the extra thermal background due to the warm components in the E-ELT - MAORY - MICADO system.

Here we assume a well-baffled system, so that a detector pixel is exposed to only the incoming radiation from the optics, telescope, sky etc. Of course, it also sits in a thermal bath at the temperature of the cryogenic detector housing (assumed 77K)

Physical Constants (CGS)

$h := 6.626 \cdot 10^{-27}$ Planck Constant $c := 2.9979 \cdot 10^{10}$ Speed of light

$k := 1.380 \cdot 10^{-16}$ Boltzmann Constant

$$L(\lambda, T, \varepsilon) := \varepsilon \cdot \frac{2 \cdot h \cdot c^2}{\lambda^5 \cdot \left(\exp\left(\frac{h \cdot c}{\lambda \cdot k \cdot T} \right) - 1 \right)}$$ Planck blackbody function

Telescope / Instrument Parameters

$telf := 18.85$ Telescope focal ratio (nominal at GIF - ESO doc)

$do := 4200 \quad di := 1200$ Outside, inside diameter of primary

$Atel := \pi \cdot \frac{do^2 - di^2}{4}$ Collecting area $\frac{Atel}{10^4} = 1.272 \times 10^3$ square meters

$narc := 0.003$ Pixel scale (primary arm)

$fr := telf \cdot \frac{15}{3838} \cdot \frac{1}{narc}$ f/ratio of "warm" beam on detector $fr = 24.557$
                          (15 μm pixels, 3838 μm per arcsec)

$st := \frac{\pi}{4} \cdot \frac{1}{(fr)^2}$ Corresponding solid angle (accurate enough here)

$A\Omega w := \left(15 \cdot 10^{-4} \right)^2 \cdot st$ Area-solid angle product receiving 'warm' radiation

$A\Omega c := \left(15 \cdot 10^{-4} \right)^2 \cdot 2 \cdot \pi$ Area-solid angle product receiving 'cold' radiation (hemisphere)

Emissivity Parameters $j := 0 .. 2$ $k := 0 .. 8$ Counters for wavelength, temperature

$\lambda c_0 := 1.25 \quad \lambda c_1 := 1.65 \quad \lambda c_2 := 2.2$ Center wavelengths for J,H,K

$T_k := 258 + 5 \cdot k$ Ambient temperature - this is -15 to +25• C

$Tc_k := 77$ Cryogenics temperature (fixed at LN2)

$$\varepsilon tel := \begin{pmatrix} 0.297 \\ 0.251 \\ 0.227 \end{pmatrix} \quad \varepsilon ma := \begin{pmatrix} 0.282 \\ 0.220 \\ 0.187 \end{pmatrix} \quad \varepsilon mic := 0.025$$
WARM JHK emissivities of telescope, MAORY, MICADO (see MICADO transmission document). This drives the background...

$\varepsilon c := 1.0$ COLD emissivity of MICADO (thermal bath has emissivity 1)

===== K Band =====

$$\lambda 1 := 2.0 \cdot 10^{-4} \qquad \lambda 2 := 2.4 \cdot 10^{-4} \qquad \lambda o := \lambda c_2 \cdot 10^{-4}$$ Wavelength Range 2.0-2.4 μm

$$\nu 1 := \frac{c}{\lambda 1} \qquad \nu 2 := \frac{c}{\lambda 2} \qquad d\nu := \nu 1 - \nu 2$$ Bandpass in Hz

$$E\gamma := h \cdot \frac{c}{\lambda o}$$ ergs per photon (at band center)

$$FZM := 6.36 \cdot 10^{-21}$$ Flux for Zero Mag in erg/cm^2/Hz (K' Interp)

$$SF := 12.7$$ Sky background in mag/square arcsec

Transmission + QE of subsystems (telescope, MAORY, MICADO see transmission document)

$$Ttel := 0.773 \qquad Tma := 0.796 \qquad Tmic := 0.530 \qquad Tatm := 0.95$$

Calculate Background from **Thermal Emission of Sky**

Sky photo-electrons / pixel /sec (constant with ambient Temp Tk)

$$\gamma sky_k := Tatm \cdot Ttel \cdot Tma \cdot Tmic \cdot \left[\left(10^{-0.4 \cdot SF} \right) \cdot \left(\frac{FZM \cdot Atel \cdot d\nu}{E\gamma} \right) \cdot narc^2 \right]$$

Calculate Background from **Thermal Emission of Telescope, Instrument, etc.**

$$\gamma tel_k := Tma \cdot Tmic \cdot \int_{\lambda 1}^{\lambda 2} L\left(\lambda, T_k, \varepsilon tel_2\right) \cdot \frac{A\Omega w}{\left(\frac{h \cdot c}{\lambda}\right)} d\lambda$$ TELESCOPE background in photo-electrons per pixel per second

$$\gamma ma_k := Tmic \cdot \int_{\lambda 1}^{\lambda 2} L\left(\lambda, T_k, \varepsilon ma_2\right) \cdot \frac{A\Omega w}{\left(\frac{h \cdot c}{\lambda}\right)} d\lambda$$ MAORY background in photo-electrons per pixel per second

$$\gamma micW_k := Tmic \cdot \int_{\lambda 1}^{\lambda 2} L\left(\lambda, T_k, \varepsilon mic\right) \cdot \frac{A\Omega w}{\left(\frac{h \cdot c}{\lambda}\right)} d\lambda$$ MICADO WARM background (window only) in photo-electrons per pixel per second

$$\gamma micC_k := Tmic \cdot \int_{\lambda 1}^{\lambda 2} L\left(\lambda, Tc_k, 1.0\right) \cdot \frac{A\Omega c}{\left(\frac{h \cdot c}{\lambda}\right)} d\lambda$$ MICADO COLD background (2π sr at Tc) in photo-electrons per pixel per second. This is VERY small for realistic Tc. For example:

$$Tc_0 = 77 \qquad \gamma micC_0 = 6.366 \times 10^{-20}$$

Plot of K BAND Background Photo-electrons per second per pixel
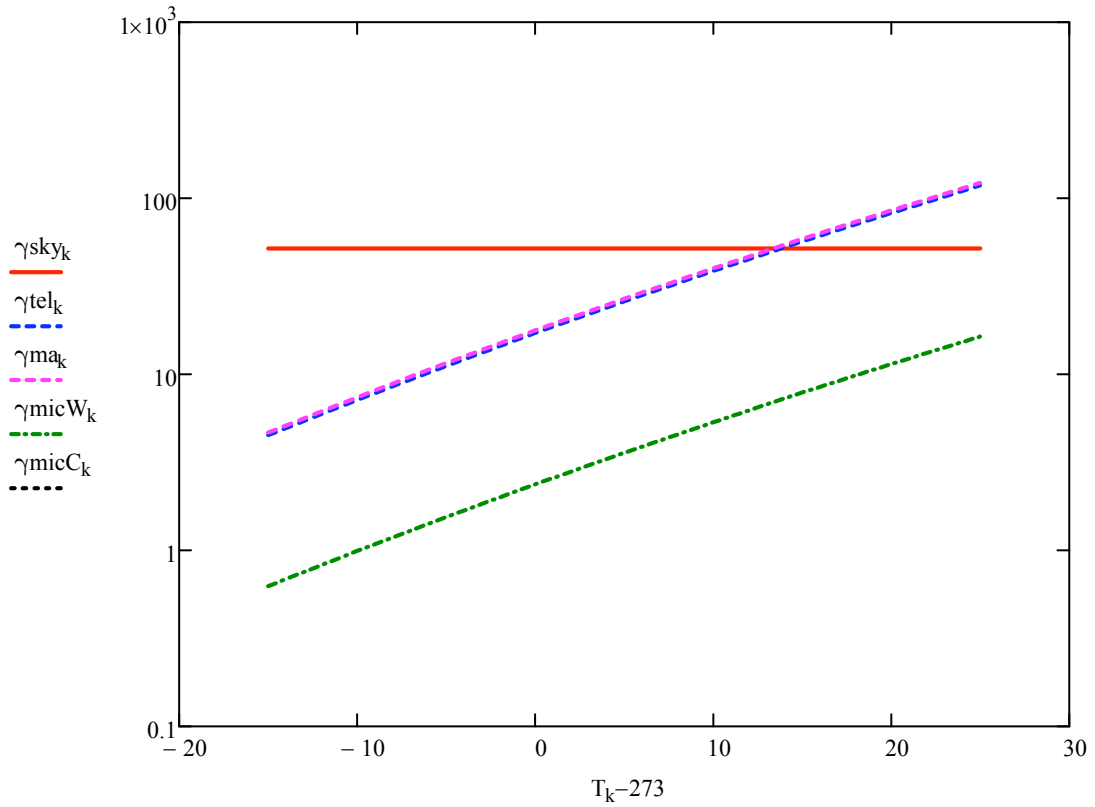
The sky, telescope, and MAORY dominate. For example:

For $\quad i := 5 \quad T_i - 273 = 10 \quad$ degrees Celsius, and the contributions are:

K Band photo-electrons from various sources (10 C ambient temperature)

$$\gamma sky_i = 51.926 \quad \text{SKY}$$

$$\gamma tel_i = 38.647 \quad \text{TELESCOPE}$$

$$\gamma ma_i = 39.997 \quad \text{MAORY}$$

$$\gamma micW_i + \gamma micC_i = 5.347 \quad \text{MICADO (warm+cold)}$$

and with respect to the telescope, MICADO's fractional contribution to background is

$$\frac{\gamma micW_i + \gamma micC_i}{\gamma tel_i} = 0.138$$

===== H Band =====

$$\lambda 1 := 1.5 \cdot 10^{-4} \qquad \lambda 2 := 1.8 \cdot 10^{-4} \qquad \lambda o := \lambda c_1 \cdot 10^{-4} \qquad \text{Wavelength Range 2.0-2.4 μm}$$

$$\nu 1 := \frac{c}{\lambda 1} \qquad \nu 2 := \frac{c}{\lambda 2} \qquad d\nu := \nu 1 - \nu 2 \qquad \text{Bandpass in Hz}$$

$$E\gamma := h \cdot \frac{c}{\lambda o} \qquad \text{ergs per photon (at band center)}$$

$$FZM := 10.20 \cdot 10^{-21} \quad \text{Flux for Zero Mag in erg/cm\^2/Hz (H Band)}$$

$$SF := 13.6 \qquad \text{Sky background in mag/square arcsec}$$

Transmission + QE of subsystems (telescope, MAORY, MICADO see transmission document)

$$Ttel := 0.749 \qquad Tma := 0.764 \qquad Tmic := 0.525 \qquad Tatm := 0.95$$

Calculate Background from **Thermal Emission of Sky**

Sky photo-electrons / pixel /sec (constant with ambient Temp Tk)

$$\gamma sky_k := Tatm \cdot Ttel \cdot Tma \cdot Tmic \cdot \left[\left(10^{-0.4 \cdot SF} \right) \cdot \left(\frac{FZM \cdot Atel \cdot d\nu}{E\gamma} \right) \cdot narc^2 \right]$$

Calculate Background from **Thermal Emission of Telescope, Instrument, etc.**

$$\gamma tel_k := Tma \cdot Tmic \cdot \int_{\lambda 1}^{\lambda 2} L(\lambda, T_k, \varepsilon tel_1) \cdot \frac{A\Omega w}{\left(\frac{h \cdot c}{\lambda} \right)} \, d\lambda \qquad \begin{array}{l}\text{TELESCOPE background in}\\ \text{photo-electrons per pixel per second}\end{array}$$

$$\gamma ma_k := Tmic \cdot \int_{\lambda 1}^{\lambda 2} L(\lambda, T_k, \varepsilon ma_1) \cdot \frac{A\Omega w}{\left(\frac{h \cdot c}{\lambda} \right)} \, d\lambda \qquad \begin{array}{l}\text{MAORY background in photo-electrons}\\ \text{per pixel per second}\end{array}$$

$$\gamma micW_k := Tmic \cdot \int_{\lambda 1}^{\lambda 2} L(\lambda, T_k, \varepsilon mic) \cdot \frac{A\Omega w}{\left(\frac{h \cdot c}{\lambda} \right)} \, d\lambda \qquad \begin{array}{l}\text{MICADO WARM background (window only)}\\ \text{in photo-electrons per pixel per second}\end{array}$$

$$\gamma micC_k := Tmic \cdot \int_{\lambda 1}^{\lambda 2} L(\lambda, Tc_k, 1.0) \cdot \frac{A\Omega c}{\left(\frac{h \cdot c}{\lambda} \right)} \, d\lambda \qquad \begin{array}{l}\text{MICADO COLD background (2π sr at Tc) in}\\ \text{photo-electrons per pixel per second. This is}\\ \text{VERY small for realistic Tc. For example:}\end{array}$$

$$Tc_0 = 77 \qquad \gamma micC_0 = 5.901 \times 10^{-31}$$

Plot of H BAND Background Photo-electrons per second per pixel
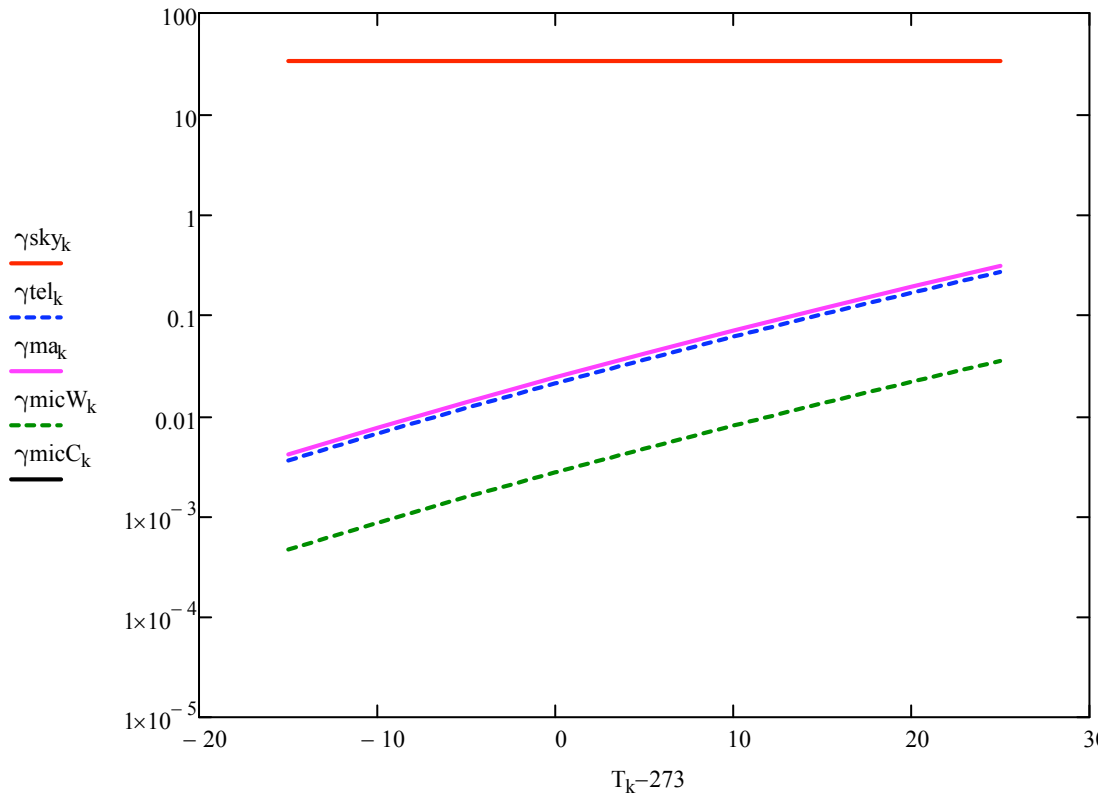
At H, the sky dominates. For example:

For $\quad i := 5 \qquad T_i - 273 = 10 \quad$ degrees Celsius, and the contributions are:

H Band photo-electrons from various sources (10 C ambient temperature)

$$\gamma sky_i = 33.488 \qquad \text{SKY}$$

$$\gamma tel_i = 0.061 \qquad \text{TELESCOPE}$$

$$\gamma ma_i = 0.07 \qquad \text{MAORY}$$

$$\gamma micW_i + \gamma micC_i = 7.989 \times 10^{-3} \quad \text{MICADO (warm+cold)}$$

and with respect to the telescope, MICADO's fractional contribution to background is

$$\frac{\gamma micW_i + \gamma micC_i}{\gamma tel_i} = 0.13$$

===== J Band =====

$\lambda1 := 1.13 \cdot 10^{-4}$ $\lambda2 := 1.37 \cdot 10^{-4}$ $\lambda o := \lambda c_0 \cdot 10^{-4}$ Wavelength Range 2.0-2.4 μm

$\nu1 := \dfrac{c}{\lambda1}$ $\nu2 := \dfrac{c}{\lambda2}$ $d\nu := \nu1 - \nu2$ Bandpass in Hz

$E\gamma := h \cdot \dfrac{c}{\lambda o}$ ergs per photon (at band center)

$FZM := 15.70 \cdot 10^{-21}$ Flux for Zero Mag in erg/cm^2/Hz (J Band)

$SF := 15.2$ Sky background in mag/square arcsec

Transmission + QE of subsystems (telescope, MAORY, MICADO see transmission document)

$Ttel := 0.703$ $Tma := 0.703$ $Tmic := 0.484$ $Tatm := 0.95$

<u>Calculate Background from **Thermal Emission of Sky**</u>

Sky photo-electrons / pixel /sec (constant with ambient Temp Tk)

$$\gamma sky_k := Tatm \cdot Ttel \cdot Tma \cdot Tmic \cdot \left[\left(10^{-0.4 \cdot SF} \right) \cdot \left(\dfrac{FZM \cdot Atel \cdot d\nu}{E\gamma} \right) \cdot narc^2 \right]$$

<u>Calculate Background from **Thermal Emission of Telescope, Instrument, etc.**</u>

$$\gamma tel_k := Tma \cdot Tmic \cdot \int_{\lambda1}^{\lambda2} L\left(\lambda, T_k, \varepsilon tel_0 \right) \cdot \dfrac{A\Omega w}{\left(\dfrac{h \cdot c}{\lambda} \right)} \, d\lambda$$ TELESCOPE background in photo-electrons per pixel per second

$$\gamma ma_k := Tmic \cdot \int_{\lambda1}^{\lambda2} L\left(\lambda, T_k, \varepsilon ma_0 \right) \cdot \dfrac{A\Omega w}{\left(\dfrac{h \cdot c}{\lambda} \right)} \, d\lambda$$ MAORY background in photo-electrons per pixel per second

$$\gamma micW_k := Tmic \cdot \int_{\lambda1}^{\lambda2} L\left(\lambda, T_k, \varepsilon mic \right) \cdot \dfrac{A\Omega w}{\left(\dfrac{h \cdot c}{\lambda} \right)} \, d\lambda$$ MICADO WARM background (window only) in photo-electrons per pixel per second

$$\gamma micC_k := Tmic \cdot \int_{\lambda1}^{\lambda2} L\left(\lambda, Tc_k, 1.0 \right) \cdot \dfrac{A\Omega c}{\left(\dfrac{h \cdot c}{\lambda} \right)} \, d\lambda$$ MICADO COLD background (2π sr at Tc) in photo-electrons per pixel per second. This is VERY small for realistic Tc. For example:

$$Tc_0 = 77 \qquad \gamma micC_0 = 6.519 \times 10^{-45}$$

Plot of J BAND Background Photo-electrons per second per pixel
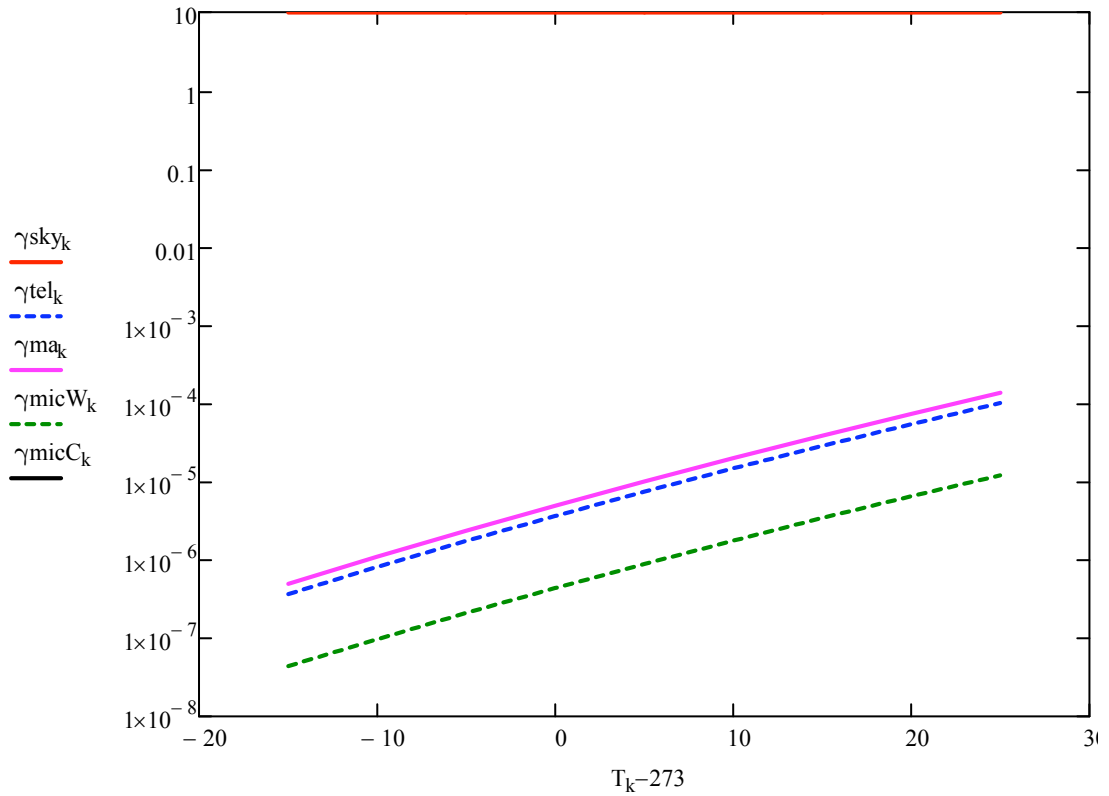
At J, the sky dominates. For example:

For $i := 5$ $\quad T_i - 273 = 10$ degrees Celsius, and the contributions are:

J Band photo-electrons from various sources (10 C ambient temperature)

$$\gamma sky_i = 9.938 \qquad \text{SKY}$$

$$\gamma tel_i = 1.475 \times 10^{-5} \quad \text{TELESCOPE}$$

$$\gamma ma_i = 1.992 \times 10^{-5} \quad \text{MAORY}$$

$$\gamma micW_i + \gamma micC_i = 1.766 \times 10^{-6} \quad \text{MICADO (warm+cold)}$$

and with respect to the telescope, MICADO's fractional contribution to background is

$$\frac{\gamma micW_i + \gamma micC_i}{\gamma tel_i} = 0.12$$